

ISTITUTO NAZIONALE DI FISICA NUCLEARE
Laboratori Nazionali di Frascati

LNF-78/25

L. Federici, M. Nardi, F. Ceradini and M. Conversi :
A LOW-COST TOTAL ABSORPTION TRACK DETECTOR
OF HIGH ENERGY PARTICLES

Estratto da :
Nuclear Instr. and Meth. 151, 103 (1978).

A LOW-COST TOTAL ABSORPTION TRACK DETECTOR OF HIGH ENERGY PARTICLES

L. FEDERICI

Laboratori Nazionali dell'INFN, Frascati, Italy

M. NARDI

Laboratori Nazionali del CNEN, Frascati, Italy

F. CERADINI and M. CONVERSI*

CERN, Geneva, Switzerland

Received 26 September 1977

A total absorption particle detector, easy to realize at a very low cost even in huge sensitive volumes, has been developed. It consists of a large number of "plastic flash chambers" alternated with plates of inert dense material in which the cascade showers develop. The chambers are sensitized by the application of a high voltage pulse which causes the chamber elementary cells to flash if they are traversed by ionizing particles. Different optical and electrical read-out systems can be applied to extract the information. The detector can be applied to measure the primary energy of impinging electrons and photons, or hadrons, up to energies of tens of GeV, or possibly more.

In the specific detector described in this article, composed of 14 chambers alternated with 0.5 cm thick Pb plates, a vidicon read-out is used to record on a triggered magnetic tape the information derivable from its ~6700 sensitive cells, which are rectangular tubes of extruded polypropylene of 3.5 mm × 5 mm cross-section. This instrument is shown to measure the primary electron energy with a (r.m.s.) accuracy $\Delta E/E = \sim (\pm 12\%)/\sqrt{E}$ (E in GeV) in the energy range 0.5–4 GeV.

As an example, the possible application of this technique to a search for "neutrino oscillations" is briefly discussed.

1. Introduction

The development of high-energy physics demands larger and larger total absorption particle detectors – often called calorimeters – the cost of which may eventually become a sizeable fraction of a large-scale installation. In this article we present a low-cost detector which, in spite of some limitations – partly related to its being normally used as a "triggered device" – also has a number of other interesting features: wide range of linear response, good energy resolution, recording of particle tracks by different possible read-out systems, modular structure and consequent flexibility, stability of performance, ruggedness, and easiness of construction.

A brief preliminary account of the work reported in the present article was given¹⁾ just one year ago. In the meantime the technique has been further developed in other laboratories, and applications to large-scale experiments in high-energy physics have been proposed²⁾. The technique itself can be regarded, on the other hand, as an improved version of that³⁾, based on the use of the "old" flash-tube chamber⁴⁾, recently investigated⁵⁾ with a view to possible applications to experiments with particle accelerators⁶⁾. In the new version

the chambers are of plastic material⁷⁾ and the detector may be defined as a "plastic flash calorimeter".

2. Essential features of the "plastic flash calorimeter"

Various types of calorimeters have been developed in recent years for application to experiments in high-energy physics. Many are of a sandwich type, consisting of plates of dense inert material alternated with "sensitive layers". The latter may be radiators of Cherenkov light⁸⁾ – if the instrument is used as a total absorption detector of high-energy electrons or photons – or scintillators⁹⁾ for more general applications. In both cases the sensitive layers enable one to sample at various depths the development of the cascade shower resulting from the impact of the primary particle (electron or photon, or any hadron). The same "sampling principle" also holds in the case of the liquid argon calorimeter developed more recently¹⁰⁾ which presents a number of improved features with respect to the classic sandwich-type detectors.

In all these examples of calorimeters, except the one exploiting the Cherenkov light which has a narrower range of applications, the quantity

* On temporary leave from the University of Rome, Italy.

sampled is the ionization deposited in each sensitive layer. The energy of the primary particle is then determined by measuring the total ionization, and the accuracy in the energy determination is therefore related to the fluctuations in the ionization measurements. These fluctuations are the result of different types of fluctuations that in general combine quadratically to give the observed energy resolution. For example, when the above-mentioned ionization sampling calorimeters are used to measure the energy of electromagnetic showers, the energy resolution depends essentially on two types of fluctuations: (1) fluctuations in the number of shower particles, related to the physics that governs the development of the shower through the elementary processes (bremsstrahlung, pair-production, etc.); (2) fluctuations in the number of delta-rays that accompany the shower particles traversing the sensitive layers. These latter fluctuations are relevant, for instance, if the sensitive layers are gas counters or multiproportional wire chambers¹¹⁾, where only a few delta-rays are produced and their ionization energy losses are nevertheless large compared to those of the minimum ionization shower particles. Instead, in a typical lead-scintillator sandwich-sampling detector, track-sampling statistics are dominant with respect to delta-ray statistics and a better energy resolution can thus be achieved.

Although of the sandwich-sampling type, the calorimeter described in this note works on a different principle in that it does not sample the ionization deposited at the various depths, but rather the number of ionizing particles. The sensitive layers of the calorimeter are in fact honeycomb-structured flash chambers⁷⁾, made of extruded plates of polypropylene. These chambers record the tracks of the traversing particles as a sequence of "flashes": the flashes associated with the luminous discharge that occurs in the tubular "chamber cells" traversed by ionizing particles. Since the discharge of one cell has no effect on the discharge of other cells, the maximum number of particles the instrument can detect is only limited by the finite space resolution due to the cells finite size ($3.5 \times 5 \text{ mm}^2$ transverse dimensions in the case of the present detector). Hence, the detector is able to measure the energy of the incoming particle by recording the total number of shower particles.

More precisely, the quantity sampled at various depths of the plastic flash calorimeter is the num-

ber of discharged cells, which is essentially proportional to just the number of shower particles present at each depth. In fact the contribution due to delta-rays can be neglected in this case, because most delta-rays are emitted at small angles and therefore go through the same cell traversed by the primary particle, whereas the few delta-rays emitted at large angles are soft electrons¹²⁾ quickly absorbed in the cell walls. The resolution in the energy measurements is dominated, therefore, by the fluctuations in the number of shower particles alone. On the other hand, by utilizing the honeycomb-structured flash chambers of extruded polypropylene⁷⁾ it is easy to realize a large number of sampling layers, each containing a very large number of tubular cells of small transversal dimensions. The quick increase in the average angular separation of the shower particles, due to their scattering in the inert plates of the detector, ensure that after a few layers the particles are sufficiently separated for there to be a reasonable probability that they will not traverse the same chamber cell, even at primary energies of several GeV, in more than one particle. The comparatively good energy resolution observed¹⁾ for the type of calorimeter being described can thus be understood, at least on this qualitative ground (see section 6 for further comments of a more quantitative nature). Improvements in this energy resolution should be obtained by exploiting all the additional information which can be derived from the knowledge of the particle tracks.

The range of applications of the plastic flash calorimeter is somewhat limited by its being normally used as a triggered device¹³⁾. This implies a sensitive time (memory of particle traversal) of at

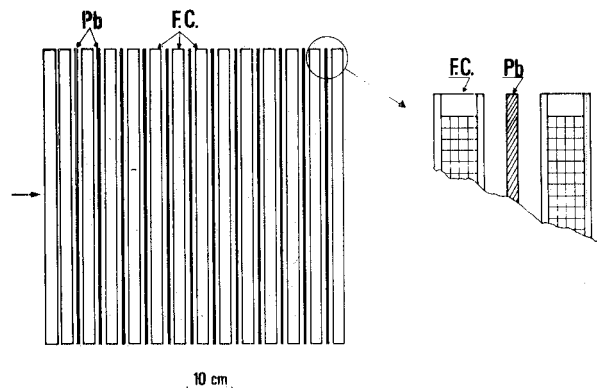


Fig. 1. Schematic side view of the detector in the "electromagnetic calorimeter" version. It consists of 14 plastic flash chambers alternated with 5 mm thick lead plates.

least a few hundred nsec: the time required to create and apply the high voltage (hv) pulse that sensitizes the chamber cells. Furthermore, the impulsive electric discharges occurring in the cells traversed by particles after the application of the high voltage pulse, are accompanied by rather long recovery-time effects which hinder the possibility of achieving trigger rates much in excess of a few per second. Nevertheless, in spite of these drawbacks, and on account of the positive features mentioned at the beginning and discussed later in this article, the device appears applicable with substantial advantages to a variety of experiments in

the fields of cosmic rays, high-energy neutrino physics, e^+e^- collisions, etc., whenever background conditions are not too severe and events need not be recorded at exceedingly high rates.

3. Description of the plastic flash calorimeter

Basically a plastic calorimeter consists of a conveniently large number of moduli, each made up of a slab of dense inert material (e.g. a metal plate) followed by a plastic chamber of approximately the same area. Multiplication and/or absorption of the incoming particles occur in the inert plates and the

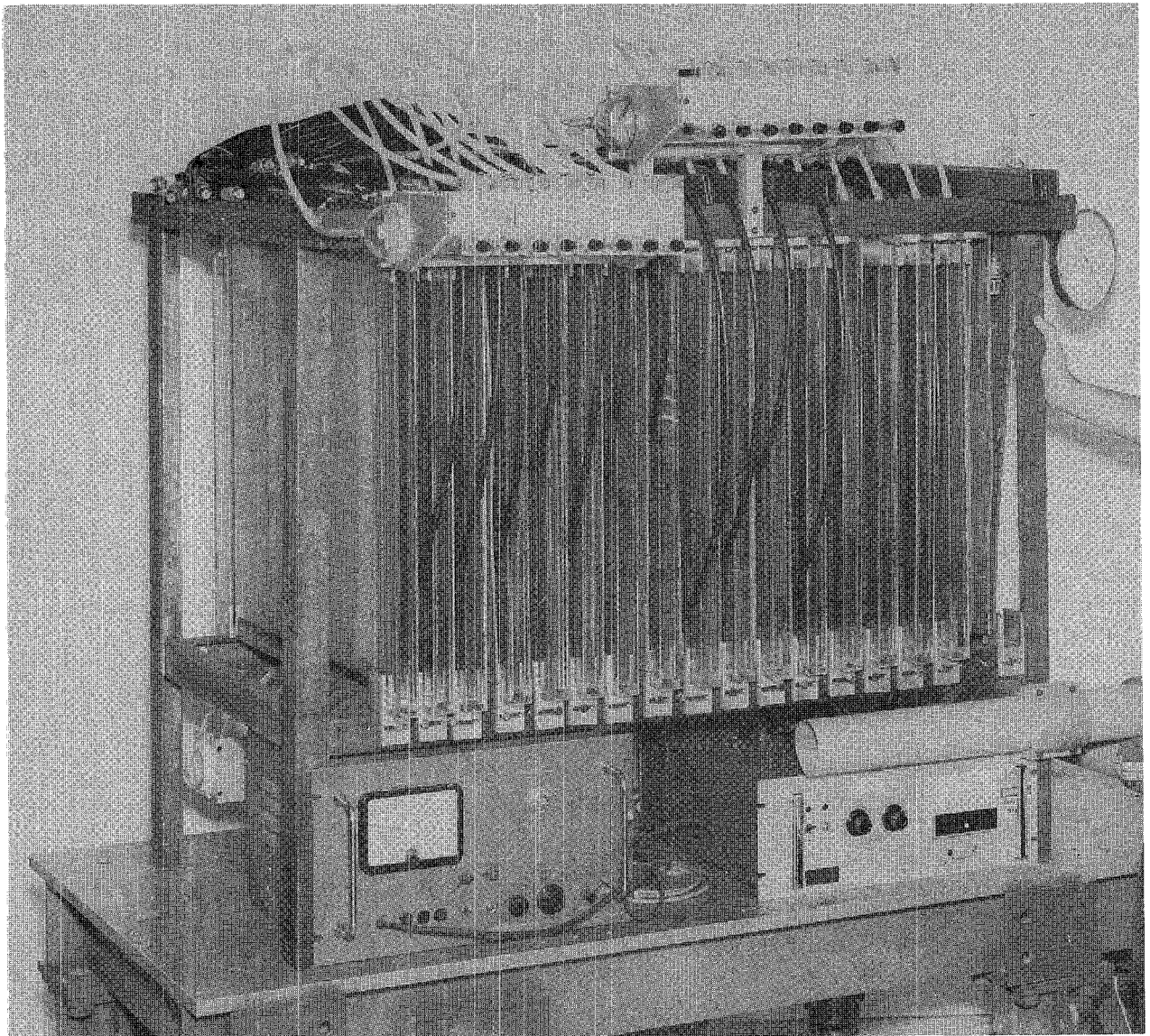


Fig. 2. General view of the plastic flash calorimeter.

particles are detected by the plastic flash chambers where their tracks are observed. As for other calorimeters of the sandwich-sampling type, thickness, positioning, kind of material and total number of inert plates, have to be chosen bearing in mind the specific application of the instrument. Thus, if the latter is intended to provide an accurate determination of the energy of a primary electron or photon in the GeV region, lead plates of, at most, one radiation length thickness, covering a total thickness of at least 10 radiation lengths, may be a reasonable choice.

These are essentially the characteristics of the type of calorimeter shown in figs. 1 and 2, which has been exposed for calibration purposes to electrons of primary energy ranging from 0.5 to 4 GeV (see section 5). Each of its twelve equal moduli consists of a 5 mm thick Pb plate followed by a honeycomb-structured plastic chamber. As shown in fig. 2 of the preceding article, the latter is made of four extruded plates of "moplen", a type of polypropylene commercially available in a variety of shapes. Each extruded plate consists of a large number of thin-walled rectangular tubes of 3.5 mm \times 5.0 mm area, in which a noble gas mixture is made to flow. These tubes are the "sensitive elements" or "cells" of the chamber, in that upon application of an intense electric field (~ 10 kV/cm) a luminous discharge occurs in the tubes which have been traversed by ionizing particles, but not in the other tubes, thus allowing one to record the particle tracks through a suitable read-out system (see next section).

Moplen was chosen as a result of a systematic investigation carried out on the behaviour of several samples of different plastic materials⁷). Among the reasons for such a choice, discussed to some extent in ref. 7, we recall here the possibility of operating a moplen chamber with good detection efficiency, even when the noble gas mixture flows through the chamber cells at a very low rate. It is believed that the rate of gas flow has to be adjusted to the rate of emission of electronegative impurities from the plastic material. During the time Δt that elapses between the instant of particle traversal and the application of the sensitizing hv pulse, these electronegative impurities may capture some of the primary ionization electrons, thus causing a reduction in the chamber detection efficiency unless the rate of noble gas mixture flow is not large enough.

In the applications of the plastic calorimeter

which is described, Δt was typically 0.4 μ s. The rate of flow of the 30/70 He/Ne noble gas mixture was about 1 l/h for each modulus. The pulse was obtained by a spark-gap controlled by a delay line.

The shape, duration, and amplitude of the hv pulse are somewhat critical, in that substantial changes with respect to the "optimal conditions" may result in spurious flashing of nearby cells not traversed by ionizing particles⁷).

4. Read-out system

The information which can be derived from the luminous discharge of the flash cells can be extracted by a number of different methods using "optical" or "electrical" read-out systems⁷). The one adopted for the measurements reported below is a "direct" optical read-out, based on the use of a silicon array target vidicon on which the detectors' image is directly focused by a telecentric set of lenses. This system, described in detail elsewhere¹⁴), is illustrated schematically in fig. 3, where the exposure of the calorimeter to the particles of a beam of known momentum is also indicated. The nature of the particles contained in this beam (electrons, muons, pions, ...) is identified by a system of scintillation and gas Cherenkov counters in association with a suitable "logic circuit" (see section 5).

The read-out system is characterized by the following peculiar features:

- 1) The magnetic writing cycle of each single frame is done in the "stop" tape position, and the tape advances step by step at the occurrence of each event, rather than running continuously as in ordinary cases. This allows a large number of events to be recorded ($\sim 10^5$) on a single magnetic tape of commercial type.
- 2) The scanning of the vidicon target by the electron gun of the analyser tube is stopped by the same trigger signal which activates the hv pulse generator of the flash chambers. At the arrival of the first beam particle selected by the "logic circuit" (fig. 3) the hv pulse generator is triggered immediately in order to sensitize the calorimeter flash chambers; whereas the scanning of the vidicon target is restarted after a delay of ~ 100 ms, large compared to the emission time of the flash light¹⁵). Essentially, the same trigger is used to advance the tape by one step after an additional delay of ~ 100 ms, long

enough to complete the scanning, with cancellation, of the vidicon target, and the recording on the magnetic tape.

Videograms of the recorded events can then be seen, at any desired time, on the TV screen of the "monitor" shown in fig. 3.

5. Results of exposure to high-energy electrons

The particular version of the plastic flash calorimeter described in section 3 is suitable for measuring the energy of primary electrons or photons incident on it with energies from a fraction of 1 GeV to several GeV. For calibration purposes, and also in order to study its behaviour when exposed to energetic particles of other types, the calorimeter was exposed to one of the secondary beams of the CERN 28 GeV Proton Synchrotron (PS). This beam contained mostly pions, with a small percentage of electrons and muons distributed in time over its 300 ms spill-out. Selection of each type of particle was achieved by a "logic circuit" elaborating the pulses from a system of scintillation and Cherenkov counters (fig. 3) as indicated below:

$$\begin{aligned} e\text{-trigger: } & S1 \cdot S2 \cdot C1 \cdot C2 \cdot S3 \cdot \bar{V}, \\ \pi\text{-trigger: } & S1 \cdot S2 \cdot \bar{C1} \cdot \bar{C2} \cdot S3 \cdot \bar{V}, \\ \mu\text{-trigger: } & S1 \cdot S2 \cdot \bar{C1} \cdot \bar{C2} \cdot S3 \cdot S4. \end{aligned}$$

The gas pressure in the Cherenkov counters was set at a value such that over the momentum range explored, from 0.5 to 4 GeV (nearly the maximum energy value of the electrons present in the beam), electrons released Cherenkov light, whereas pions and muons did not.

Systematic calibration measurements were made shooting into the calorimeter electrons from 0.5 to 4 GeV/c momentum, in steps of 0.5 GeV/c. The videograms corresponding to each machine pulse were recorded on magnetic tape as previously explained (section 4). They were later analysed so as to extract from each videogram the total numbers of discharged chamber cells, N_d . Fig. 4 shows distributions of these numbers based on samples of some hundred of events recorded at each selected energy. From these distributions one can derive the average number of discharged cells, \bar{N}_d , and the r.m.s. deviation from this average at each primary energy, E .

The energy dependence of \bar{N}_d and of the r.m.s. energy resolution, $\Delta E/E$, are given in fig. 5 and

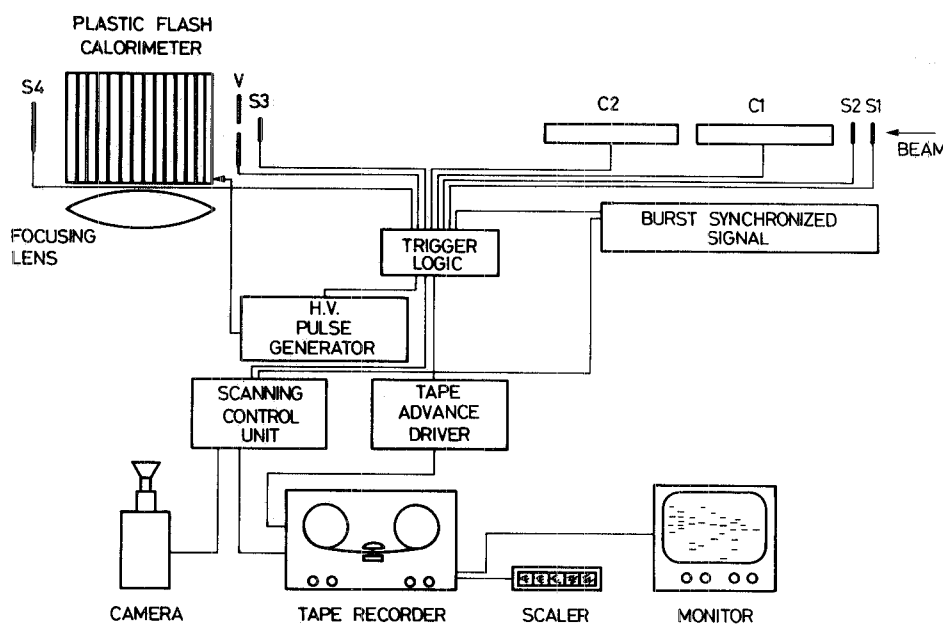


Fig. 3. Schematic layout of the trigger counters and of the read-out system. S1, S2, S3, S4 and V are plastic scintillators, C1 and C2 are gas Cherenkov counters. The light emitted from the discharged cells is focused by a large lens on the vidicon camera objective. A signal synchronized with the accelerator burst is used to reset the scanning of the vidicon target. The pulse of the trigger logic is used to sensitize the plastic flash chambers, to enable the scanning of the vidicon target and to advance the magnetic tape. The image recorded on magnetic tape can be displayed on the TV monitor. The total number of discharged cells is counted by a scaler.

fig. 6, respectively. It is seen from these figures that over the energy range explored experimentally:

- 1) The instrument has a nearly linear response, \bar{N}_d being essentially proportional to E .
- 2) The resolution in the measurement of the primary energy E is given approximately by

$$\Delta E/E = \sim (12\%)/\sqrt{E},$$

when E is measured in GeV.

In connection with (1) above, we wish to point out the possibility of a quick measurement of the energy E , and therefore that of using the shower detector as an "energy trigger". Since the number of discharged cells (N_d) is nearly proportional to the primary electron energy E , it is possible to

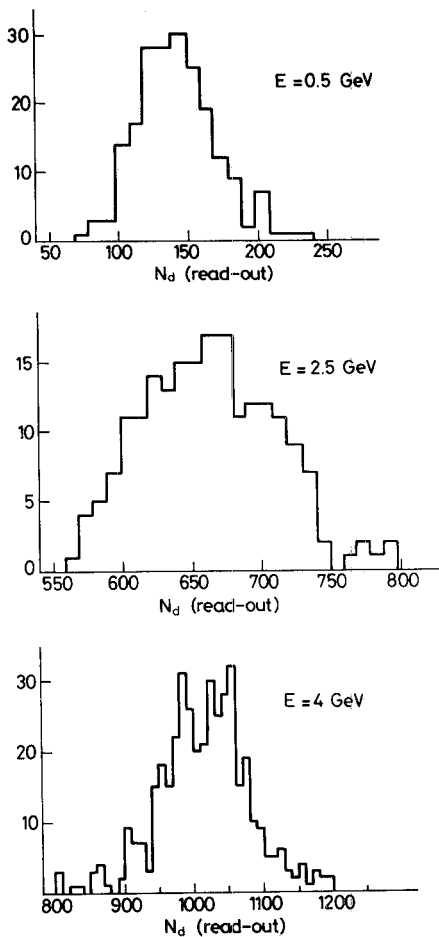


Fig. 4. Examples of distributions of the number of discharged cells, for primary electrons of different energies. The entries of the histograms are the direct outputs of the read-out system. The actual number of discharged cells N_d , is obtained by dividing this output by the average number of scanlines per cell, which is equal to 3.

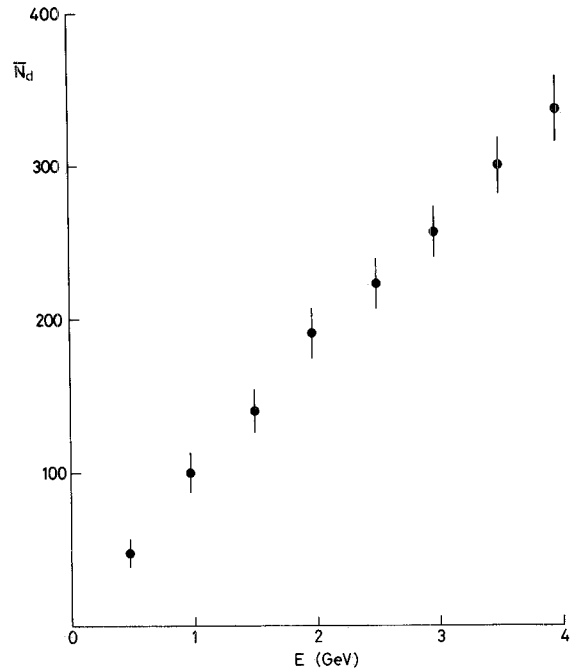


Fig. 5. Energy dependence of the average total number of discharged cells \bar{N}_d , for primary electrons of energy from 0.5 to 4.0 GeV.

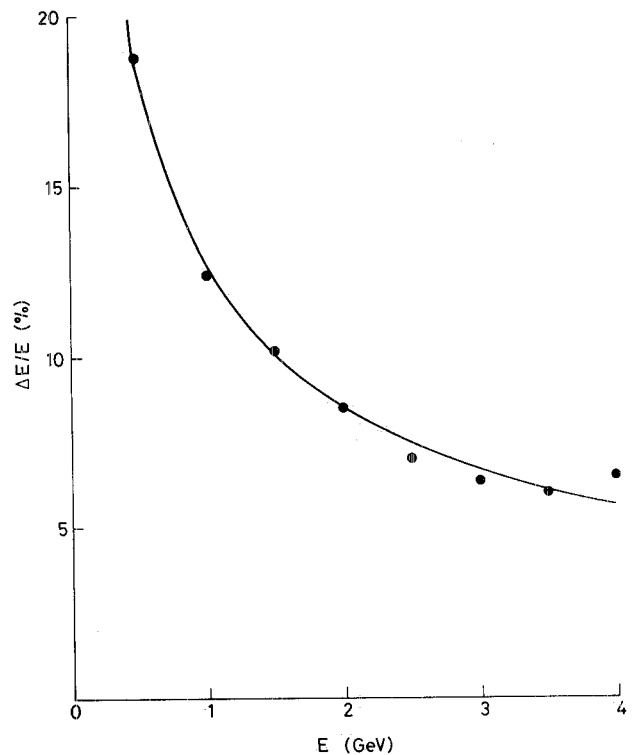


Fig. 6. Energy dependence of the r.m.s. energy resolution, $\Delta E/E$, for primary electrons of energy from 0.5 to 4.0 GeV. The data are fitted with an $a/\sqrt{E} + b$ curve ($b \ll a$).

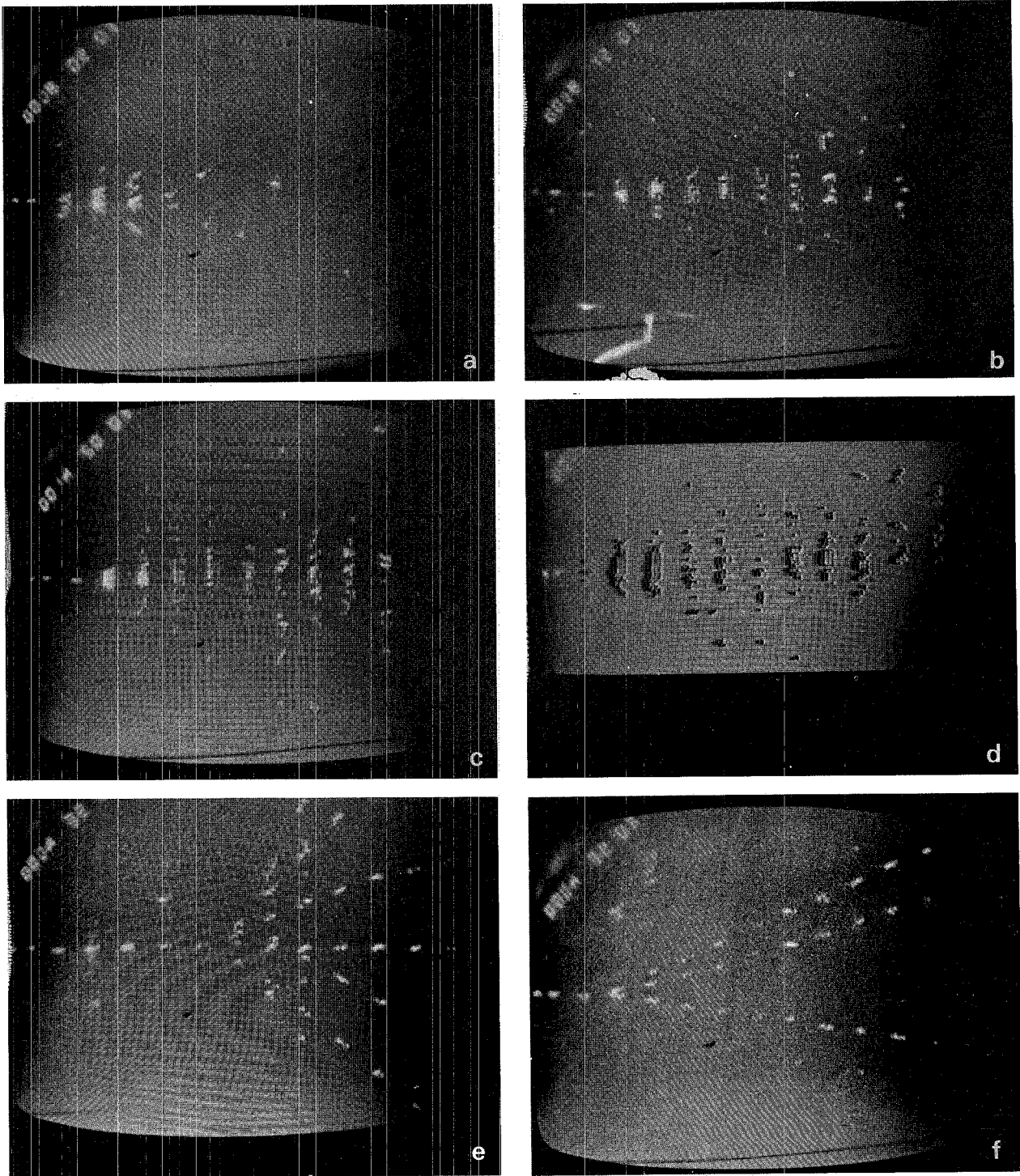


Fig. 7. Examples of videograms recorded by triggering the detector with electrons and pions of different energies. Videograms a, b, c, d, refer to electrons of 0.5, 1.5, 3.0, 4.0 GeV/c, respectively. Videograms e and f refer to pions of 3.0 and

4.0 GeV/c, respectively. Muons are promptly recognized as they give straight tracks through the detector [see fig. 2a in ref. 1].

measure this energy merely by summing up the signals of the electric probes which can be attached to the chamber cells. In the case of huge detectors containing an exceedingly large number of sensitive cells, it may be convenient to avoid the installation of so many probes and wires, and therefore to measure the energy E by some photocell receiving the total light from the discharged chamber cells. Indeed, by extrapolating to the flash chambers results known for the neon flash-tubes¹⁵⁾ one expects that the total light is approximately proportional to N_d and hence to E . Both the above-mentioned electrical and optical read-out choices appear extremely simple methods of obtaining the energy deposited in the calorimeter quickly, and of selecting events that involve energies in excess of any prefixed value promptly.

In connection with (2), we recall the possibility of improving the energy resolution of our detector by exploiting all the additional information derivable from the knowledge of the particle tracks. Examples of videograms for different particles of various energies are reported in fig. 7 to give a feeling on the level of "pattern recognition" derivable from such an additional information.

6. Interpretation of experimental results

For the interpretation of the experimental results we first recall (see also section 2) that the plastic flash calorimeter is not a total absorption detector of the usual "proportional type" but it gives a digital response. This response is related to the spatial development of the shower in the detector.

For high-energy primary electrons or photons the opening angle of a secondary particle of energy E_s is of the order m/E_s and the secondaries are not completely resolved unless $(m/E_s)d$ (where d is the sampling period) is large compared with the spatial resolution of the detector. However, the energy deposited by unresolved tracks in the first few radiation lengths is a small fraction of the primary energy, E_0 , and the number of low energy secondaries is still in good approximation proportional to E_0 . When the energy degradation becomes effective for the spatial separation of the secondaries, the sum of many digital signals originates a response proportional to E_0 .

To ensure a linear behaviour, two conditions should be fulfilled:

- 1) good containment of the electromagnetic shower in the detector;

- 2) average density of secondaries per traversed sensitive cell close to 1, or smaller.

The results presented in the previous section indicate that the above conditions are both fulfilled for primary energies up to 4 GeV.

The results of our measurements were then compared with the expectations from a detailed Monte Carlo simulation of the shower development in the detector¹⁶⁾. The particles are followed up in this simulation until they reach a "limit total energy" of 1.3 MeV, corresponding to the average total energy required, for an electron emerging from the lead plates, to penetrate the chamber cells.

We list the following relevant results derived from the above-mentioned Monte Carlo calculation:

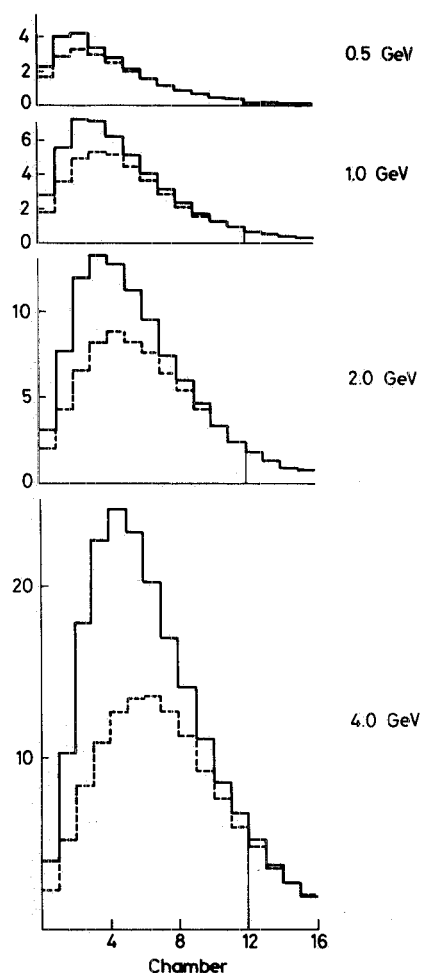


Fig. 8. Monte Carlo distributions of the number of secondaries (full line) and of discharged cells (dashed line) as a function of the depth in the plastic flash calorimeter. The dashed line is normalized to 0.8 secondaries per traversed cell at large depth.

- 1) For an infinite dimensions detector, the number N_s of sampled secondaries with total energy greater than 1.3 MeV is found to be proportional to the primary energy E_0 : $N_s \approx 52 E_0$, if E_0 is expressed in GeV¹⁷).
- 2) For the specific detector of fig. 1, the back and lateral leakages introduce a small saturation effect, of the order of 10% at $E_0 = 4$ GeV.
- 3) The effect of the unresolved secondaries is as shown in fig. 8, where the numbers of secondaries and of discharged cells, as de-

rived from the Monte Carlo simulation, are plotted as a function of the detector depth. The number of discharged cells is normalized to the number of secondaries at large depths, where all tracks are resolved. The computed asymptotic density of secondaries is ~ 0.8 per traversed tubular cell. This factor is energy independent and contains the chamber efficiency and the sensitive cell packing fraction¹⁸).

In figs. 9 and 10 the experimental data are compared with the Monte Carlo results. The computed

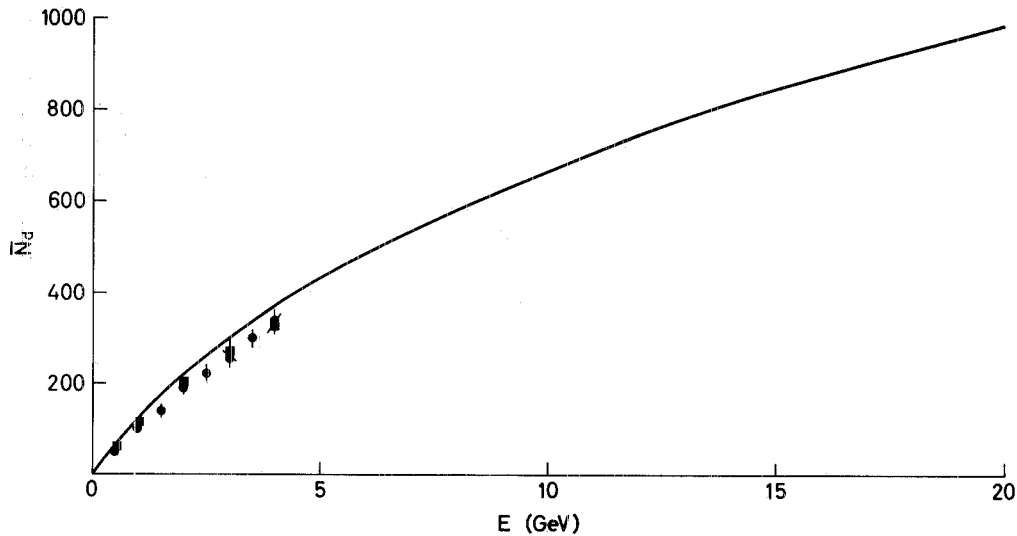


Fig. 9. Comparison of the average total number of discharged cells \bar{N}_d , as obtained from the experimental test (●) and from the Monte Carlo simulation (■) for 12 plastic flash chambers. The full line represents the Monte Carlo extrapolation to higher energies for 16 chambers and is therefore above the experimental points, as expected.

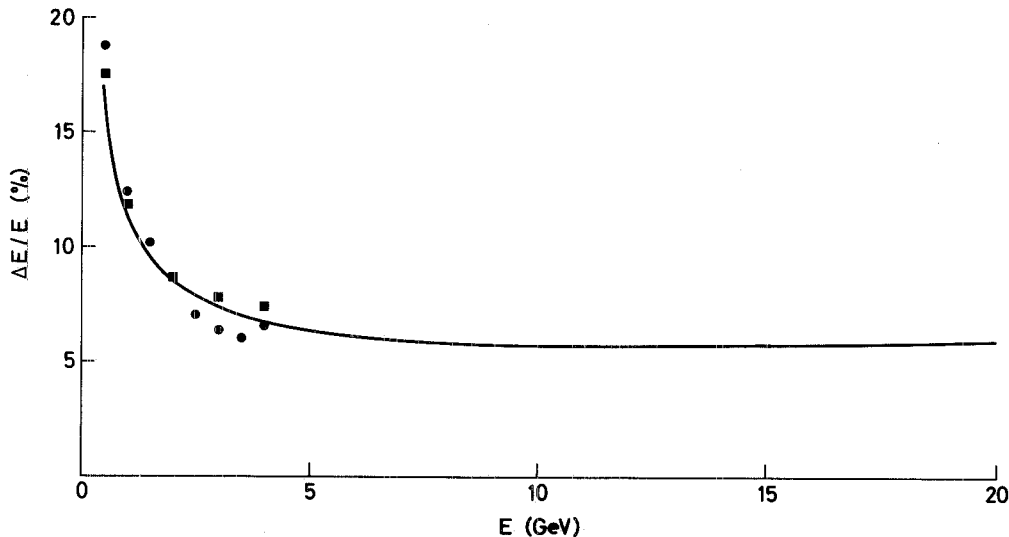


Fig. 10. Comparison of the r.m.s. energy resolution $\Delta E/E$, as obtained from the experimental test (●) and from the Monte Carlo simulation (■) for 12 plastic flash chambers. The full line represents the Monte Carlo extrapolation to higher energies for 16 chambers.

average total number of discharged cells (\bar{N}_d) and r.m.s. energy resolution ($\Delta E/E$) both show a saturation effect slightly more pronounced than in the real detector. This may be due to the fact that the chambers can be sensitive to secondary electrons of energy somewhat smaller than that of the Monte Carlo threshold. These secondaries, being of low energy, are completely resolved.

Extrapolation has been made by the Monte Carlo simulation, up to 20 GeV, for a calorimeter identical to the real one, but consisting of 16 moduli (~ 16 radiation lengths), thus ensuring a better containment of the showers. The extrapolated results are also shown in figs. 9 and 10. These results are consistent with those reported by Walker et al.²⁾ It is likely that increasing the number of moduli and their distance would extend the range of application of the instrument to the 100 GeV region.

7. Results and interpretation of a hadron test

After a change in its modular structure, the same detector was exposed for a short run to the same beam, but selecting hadrons (mostly pions) of momentum from 1 to 4 GeV/c rather than electrons. The modular structure was, in this case, one four-layer plastic chamber as before, and a 5 cm thick Fe plate, repeated in 8 moduli totalling about 2.4 interaction lengths. The hadron selection was achieved by triggering the chambers by the appropriate logic signal, as previously explained (section 5).

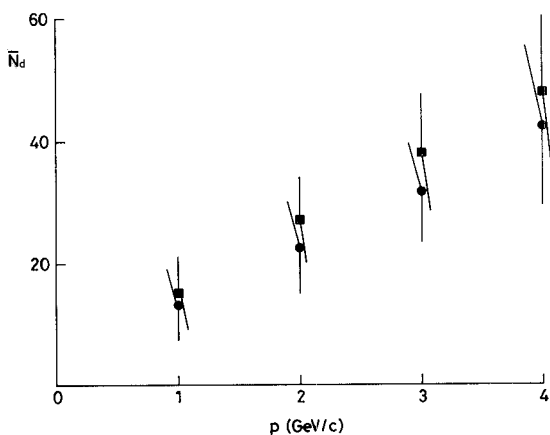


Fig. 11. Momentum dependence of the average total number of discharged cells \bar{N}_d , (●) for negative pions interacting in a plastic flash chamber detector made of eight chambers alternated with 5 cm thick iron plates. Results obtained by a Monte Carlo simulation of the hadronic cascade are also shown (■).

The experimental results of this test are presented in fig. 11.

A comparison with other hadron calorimeters is difficult because in the case of this "hadron test": (1) there are few data in the energy interval explored, and (2) the total detector thickness is not large enough to ensure a good containment of the hadronic shower at high energies.

The data were again compared with the results of a Monte Carlo calculation, this time utilizing an existing program for the simulation of the hadronic cascade¹⁹⁾, implemented for the electromagnetic component by the program of the simulation quoted in ref. 16.

In this case, the opening angle of the secondaries is larger than for electrons (see figs. 7e and 7f) and the ratio between the number of sampled secondaries and the number of discharged cells is less sensitive to the primary energy than in the case of electrons (see fig. 12). The dashed lines in fig. 12 are normalized at large depths to completely resolved secondaries, as in the previous case of primary electrons.

Comparing the results for pions and electrons

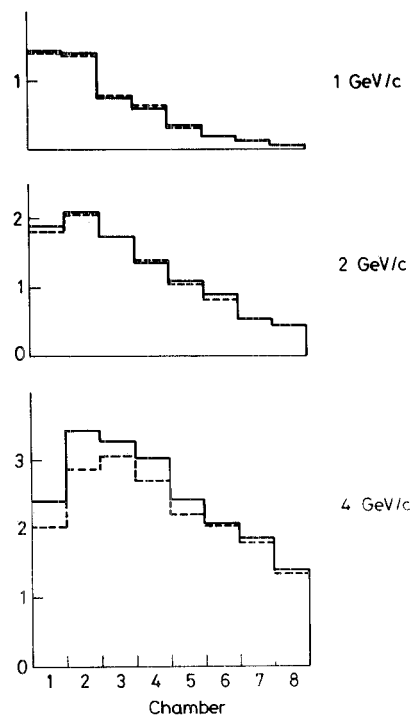


Fig. 12. Monte Carlo distributions of the number of secondaries (full line) and of discharged cells (dashed line) as a function of the depth in the plastic flash chamber detector used during the hadron test. The dashed line distribution is normalized as in the case of electrons.

we can estimate, with the help of the Monte Carlo, the rejection factor against pions for the “electromagnetic calorimeter”. The results are shown in fig. 13. Setting a threshold cut at two standard deviations the number of pions which can simulate an electron is of the order of 1% at energies greater than 1 GeV.

Extrapolation to higher energies made for a detector which has the same structure as our “hadron calorimeter” but a total thickness of 150 cm of Fe, leads to results for π^- at 5, 10, and 20 GeV/c that are consistent with those obtained by sandwich-sampling calorimeters of standard type²⁰). Over the energy range covered by our simulation, this detector has a linear response, with a resolution of about 16% at 10 GeV, if moduli with 5 cm Fe plates are employed.

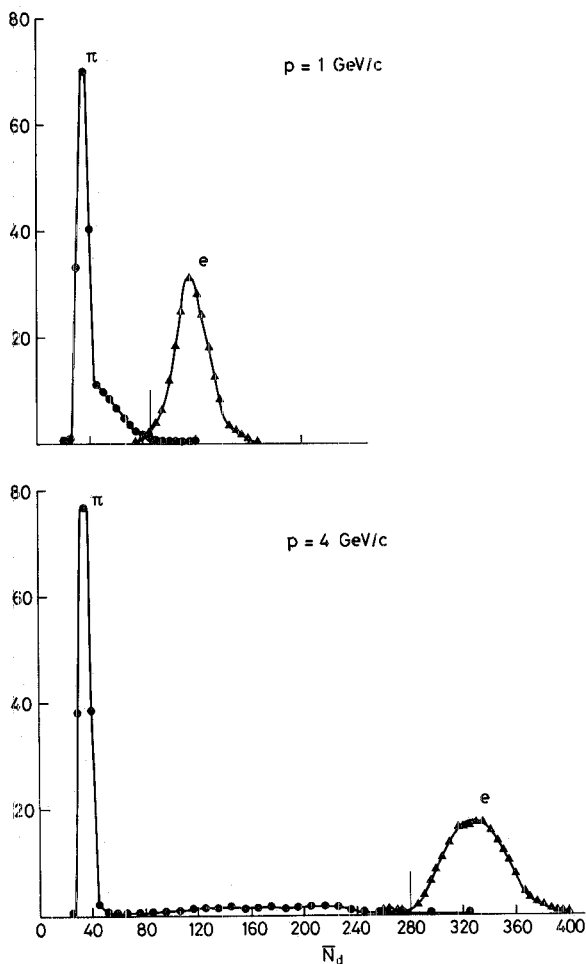


Fig. 13. Monte Carlo distributions of the total number of discharged cells for electrons and pions of the same momentum for the calorimeter of figs 1 and 2. In the momentum range 1–4 GeV/c, the rejection factor against hadrons is about 100.

8. Example of application: search for neutrino oscillations

Examples of application of the plastic flash calorimeter to high-energy physics have already been given through recent proposals from various laboratories²). We wish to add here another example – the application to a search for “neutrino oscillations” – in which the technique seems to meet particularly well the requirements of installing a huge neutrino detector at a reasonable cost, far away from the laboratory where the high-energy neutrino beam is produced.

The possibility that neutrinos “oscillate” between different states was first suggested a long time ago by Pontecorvo²¹), but there has recently been a revival of interest for such a possibility that justifies some effort to push further the present upper limit for the existence of this phenomenon^{22,23}). Even though the effect of possible $\nu_\mu \leftrightarrow \nu_e$ oscillations decreases with the square root of the primary neutrino energy²³), some authors have yet considered that it might be convenient, for the purpose, to exploit a high-energy proton synchrotron as the source of a high-intensity neutrino beam²⁴). Under this assumption a comparatively simple method to search for an effect due to possible $\nu_\mu \leftrightarrow \nu_e$ oscillations is sketched in fig. 14.

We assume that a huge plastic flash calorimeter (PFC) containing many tons of dense material be placed at a distance D of many km from the neutrino facility (NF) of a high-energy accelerator laboratory. An rf signal transmitted from this laboratory just before the start of the machine spill-out,

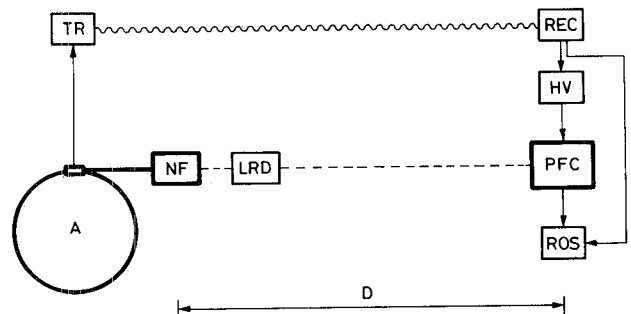


Fig. 14. Schematic representation of a possible search for high-energy “neutrino oscillations” exploiting the technique described in this article. (A: accelerator; NF: neutrino facility; LRD: local reference detector; PFC: plastic flash calorimeter; TR: transmitter; REC: receiver; HV: high voltage pulse generator; ROS: read-out system.) The figure is only indicative: large quantities of dense matter may also be present between the two stations, as will certainly be the case²⁵) for very large distances D .

is received at the place of PFC and is used to trigger the generator that applies the sensitizing hv pulse to PFC.

In order to clarify the main features of the proposed method, we list the following series of linked remarks:

- a) Practically only neutrinos reach the plastic flash calorimeter (PFC) if this is placed at a large distance from the edge of the dense material possibly encountered by the beam. In fact muons, in equilibrium with the parent neutrinos while traversing dense matter, emerge from the latter with sufficient angular spread – due to Coulomb scattering – to miss PFC.
- b) As a consequence of (a) above, the machine (which is assumed to give bursts at a rate of 1 every few seconds) can be operated with a short spill-out (say, some $10 \mu\text{s}$). In fact, in spite of the unfavourable duty cycle associated with this short spill-out, the average time distance between charged particles traversing PFC during the machine spill-out is large compared with the PFC sensitive time (typically $\sim 1 \mu\text{s}$) and no background tracks will be detected by PFC.
- c) As a consequence of (b) above, the PFC chambers can be operated in the “synchronized mode”⁷⁾, i.e. by letting the rf signal transmitted from the laboratory directly trigger the hv pulse generator which sensitizes the PFC chambers. In fact it should not be difficult to operate a large number of big flash-chambers in synchronized mode, with sensitizing hv pulses as short as some $10 \mu\text{s}$ ¹³⁾.
- d) As a consequence of (c) above, no triggering counters or other equipment are needed at the place where PFC is installed, except the hv pulse generator that sensitizes the chambers and the read-out system required either to record the information from PFC in place, or to transmit it back to the laboratory.
- e) As a consequence of (d) above, a huge “fine grain” PFC of some 100 m^2 detecting area can be conceived, and realized at a still reasonable cost, so as to have a favourable detection rate of neutrino events in PFC, even at large distances D between the laboratory and PFC, with all the information that only a multitrack detector can give. This information could be recorded by video-optical read-

out systems of the type described in section 4.

- f) As a consequence of the fine grain mentioned in (e) above, one can minimize the difficulty of distinguishing two types of electromagnetic showers: those originated from electrons, possibly due to ν_e , and those originated from γ -rays resulting from decay of π^0 mesons produced in ν_μ -induced neutral current events. These events do not have the characteristic “muon signature” and might therefore simulate ν_e -induced events.

Nevertheless, since the neutrino beam certainly contains some fraction of ν_e from K decay to electrons, it is essential to have a “local reference detector” (LRD, preferably similar to PFC, but smaller) installed near the exit of NF. Then the effect of possible neutrino oscillations would be searched for in a variation of the ratio between the numbers of events involving electromagnetic showers with and without an associated μ , as measured by PCF and LRD.

We are greatly indebted to Dr. F. Lacava for his many calculations which were essential for the present work. We wish to thank, furthermore, Mr. O. Ciaffoni, Dr. S. Gentile and Mr. A. Pecchi for the pictures of the videograms and Dr. R. Santonico for critical discussions.

References

- 1) M. Conversi, L. Federici, S. Gentile and M. Nardi, CERN EP Int. Report 76-20 (1976).
- 2) J. K. Walker et al., Proposal for a new detector at Fermilab (1977); E. M. Friedlander, L. N. Hand et al., A proposal to search for short-lived particles produced by antineutrinos and neutrinos, Fermilab Proposal No. 553 (1977); also, private communications to one of us (M.C.) from B. A. Dolgoshein, G. Salvini, B. Stella, H. Ticho and F. Villa.
- 3) G. Brocco, Thesis (University of Rome, 1973) (unpublished). The results of this work have been partly reported in a 1973 survey report on the flash chamber technique: M. Conversi, Nuovo Cim. 3 (1973) 3. C. Bemporad, M. Calvetti et al., Proc. Int. Conf. on *Instrumentation for high-energy physics* (Frascati, 1973) p. 193, developed a large flash-tube shower detector, now installed around one of the colliding-beam straight sections of ADONE, the Frascati e^+e^- 3 GeV storage ring.
- 4) M. Conversi and A. Gozzini, Nuovo Cim. 2 (1955) 189; G. Barsanti et al., Proc. CERN Symp. on *High-energy accelerators and pion physics* (CERN, Geneva, 1956) vol. 2, p. 55.
- 5) J. E. Chaney, J. M. Breare and I. D. Tait, Nucl. Instr. and

- Meth. **125** (1975) 189; J. Breare et al., Nucl. Instr. and Meth. **143** (1977) 41 and 49; C. Bemporad, M. Calvetti, F. Costantini, C. Guidi and P. Lariccia, Proc. Int. Conf. on *Instrumentation for high-energy physics*, (Frascati, 1973) p. 193.
- 6) For experiments with particle accelerators, the standard neon flash tubes used in cosmic-ray research are in general much too slow. Methods to decrease their sensitive and recovery times have been developed, however, in recent years, in various laboratories (see ref. 7 of preceding article in this issue).
- 7) See preceding article in this issue.
- 8) C. A. Heusch and C. Y. Prescott, Report CTSL 41 (1967).
- 9) V. C. Murzin, Progr. Elem. Part. Cosmic Ray Phys. **9** (1967) 247; G. Barbiellini, B. Borgia, M. Conversi and R. Santonico, Atti Acc. Naz. Lincei **44** (1968) 233; W. V. Jones, K. Pinkau, U. Pollvogt and H. Schmidt, Nucl. Instr. and Meth. **72** (1969) 173; J. Engler et al., Nucl. Instr. and Meth. **106** (1973) 189; B. C. Barish et al., Nucl. Instr. and Meth. **116** (1974) 413; **130** (1975) 49.
- 10) W. J. Willis and V. Radeka, Nucl. Instr. and Meth. **120** (1974) 221; G. Knies and D. Neuffer, Nucl. Instr. and Meth. **120** (1974) 1; J. Engler et al., Nucl. Instr. and Meth. **120** (1974) 157; S. E. Derenzo, Nucl. Instr. and Meth. **122** (1974) 319.
- 11) T. Katsura et al., Nucl. Instr. and Meth. **105** (1972) 245.
- 12) With good approximation the kinetic energy of a knock-on electron emitted at an angle $\theta > \sim 20^\circ$ is given by $E = 2mc^2 \cot^2 \theta$ (m = electron mass).
- 13) In applications to experiments with high-energy particle accelerators (see section 8, for an example), it should be possible to operate the calorimeter flash-chambers also in the "synchronized mode" (ref. 7), i.e. by using sensitizing hv pulses occurring just before the start of the machine pulse and lasting (possibly) as long as the machine spill-out. See I. Mannelli and E. Rosso, CERN Report EF/ER/mk (1977) for preliminary tests on this mode of operation with 1 ms long pulses. These and further tests by D. Miller (private communication) are being made in view of the possibility of utilizing flash-cells installed inside a large bubble chamber as time detectors of the particle traversals.
- 14) M. Nardi, O. Ciaffoni, L. Federici and A. Pecchi, LNF Internal Report, in preparation (Frascati, 1977).
- 15) H. Coxell, M. A. Meyer, P. S. Scull and A. W. Wolfendale, Nuovo Cim. Suppl. **21** (1961) 7. Investigations on neon-filled glass flash-tubes indicate that the intensity of the emitted light falls with a time constant of $5 \mu\text{s}$. Moreover, the light emitted from n flash-tubes is found to be a nearly linear function of n .
- 16) This Monte Carlo simulation, developed by F. Lacava (LNF Internal Report, in preparation) takes into account all known corrections and predicts results in good agreement with those derived from pre-existing treatments of the electromagnetic cascade [H. Messel and D. F. Crawford, *Electron-photon shower distribution function* (Pergamon Press, London, 1970); H. A. Nagel, Z. Physik **186** (1965) 319].
- 17) This result agrees well with the simple formula (ref. 11) $N_s = KE/t$, where t is the thickness of the radiator plates and K is a constant for a given material and a given energy threshold of the secondary particles.
- 18) The over-all cell efficiency introduced in the Monte Carlo is $\sim 20\%$ smaller than that measured ($\sim 85\%$), to compensate for an over-estimation of the number of traversed cells in the case of inclined tracks, due to the dimensions of the cell walls.
- 19) A. Grant, Nucl. Instr. and Meth. **131** (1975) 167. We wish to thank Doctor A. Grant for making available to us his simulation program. We wish also to thank Prof. G. Salvini and Dr. B. Stella for their stimulating discussions on the possibility of applying our technique to detect high-energy hadron cascades. For references to previous Monte Carlo treatments of the hadronic cascade, see also A. Baroncelli, Nucl. Instr. and Meth. **118** (1974) 445.
- 20) B. C. Barish et al., Nucl. Instr. and Meth. **116** (1974) 413; **130** (1975) 49.
- 21) B. Pontecorvo, Zh. Exsper. Teor. Fiz. (USSR) **33** (1957) 549; **34** (1958) 247. Soviet Phys. JETP **6** (1958) 429; **7** (1958) 172.
- 22) See, for instance: E. Bellotti, D. Cavalli, E. Fiorini and M. Rollier, Nuovo Cim. Lett. **17** (1976) 553.
- 23) See, for instance: S. M. Bilenky and B. Pontecorvo, Proc. 18th Int. Conf. on *high-energy physics*, Tbilisi, 1976 (JINR, Dubna, 1976) vol. 2, p. B122.
- 24) See, for instance: A. K. Mann and H. Primakoff, University of Pennsylvania Report (16 June 1976); M. Baldo-Ceolin et al., Proposal to search for neutrino oscillations at CERN SPS, CERN/SPSC/76-92/P 77 (1976). See also J. K. Walker, ref. 2, p. 11; E. Egelman et al., Proposal of 17/1/1977 submitted to Brookhaven National Laboratory.
- 25) A. K. Mann and H. Primakoff, *loc. cit.*